cause our data are at large "superheating," a quantitative comparison must await either equation-of-state data in metastable states or further lifetime measurements without the complication of a fill hole. We cannot now state whether the abruptness of the decrease in lifetimes is in agreement with nucleation theory or results from another source such as the onset of large scale instability.

We *never* saw evidence of metastability when $\rho_{mean}$ had the values $0.68\rho_c$, $0.90\rho_c$, $0.94\rho_c$, $1.02\rho_c$, and $1.05\rho_c$. The observations at $0.68\rho_c$, $0.90\rho_c$, and $0.94\rho_c$ imply that there is no barrier to nucleation of a droplet in the calorimeter, a situation which is expected if $He^3$ wets the walls of the calorimeter. The observations at $1.02\rho_c$ and $1.05\rho_c$ lead us to infer that very near $T_c$ the density at the top of the fill tube was less than $\rho_c$. (The linear model predicts that metastability will not occur in our calorimeter if $\rho_{mean} \leq 1.064\rho_c$ and wetting occurs.)

To summarize, we have reported the comparative ease of obtaining metastable thermodynamic states of $He^3$ and measuring their properties. We find that specific heat is continuous at the onset of metastability. Near the critical point the range of metastable states changes in qualitative agreement with a calculation showing a decrease in the rate of homogeneous nucleation. A detailed test of nucleation rates should be possible with further measurements of this type.

We are grateful to Dr. F. Gasparini who constructed much of the equipment used, and to P. Kreisman who purified the $He^3$.

†Work supported in part by National Science Foundation Grant No. GP 14431.

*Present address: Physics Department, Stanford University, Stanford, Calif. 94305.

[1]K. L. Wismer, J. Phys. Chem. 26, 300 (1922).

[2]A. T. J. Hayward, Nature 202, 481 (1964).

[3]P. Schofield, J. D. Litster, and J. T. Ho, Phys. Rev. Lett. 23, 1098 (1969).

[4]G. R. Brown and H. Meyer, Bull. Amer. Phys. Soc. 16, 638 (1971).

[5]M. R. Moldover, Phys. Rev. 182, 342 (1969).

[6]A. F. Andreev, Zh. Eksp. Teor. Fiz. 45, 2064 (1963) [Sov. Phys. JETP 18, 1415 (1964)].

[7]M. E. Fisher, Physics (Long Is. City, N.Y.) 3, 255 (1967).

[8]A. E. Sandström, *Cosmic Ray Physics* (Wiley, New York, 1965), p. 3.

[9]B. Wallace, Jr., and H. Meyer, Phys. Rev. A 2, 1563, 1610 (1970). Our qualitative conclusions would be unchanged had we used the critical isotherm or critical isochore derived from the multiparameter fit of all the Wallace and Meyer data to the equation of state of M. Vicentini-Missoni, J. M. H. Levelt Sengers, and M. S. Green, J. Res. Nat. Bur. Stand., Sect. A 73, 563 (1969). The latter equation of state has three coefficients and two exponents. It requires the introduction of a sixth parameter for extrapolation into the metastable region.

[10]A. Eggington, C. S. Kiang, D. Stauffer, and G. H. Walker, Phys. Rev. Lett. 26, 820 (1971).

# Nonlinear Electron-Cyclotron Drift Instability and Turbulence

D. W. Forslund, R. L. Morse, and C. W. Nielson

*Los Alamos Scientific Laboratory, University of California, Los Alamos, New Mexico 87544*

(Received 13 September 1971)

The cross-field anomalous resistivity due to the electron-cyclotron drift instability is shown to persist in the nonlinear regime as a result of mechanisms which depend critically on the magnitude of the magnetic field.

The nonlinear development of current-driven electron-cyclotron turbulence perpendicular to a background magnetic field[1,2] is important for understanding the anomalous resistance observed in collisionless-shock experiments.[3] Based on the results of numerical simulations, we outline a model of the strong turbulence which is quite different from the picture of Lampe *et al.*[4] and is in disagreement with many of their conclusions, particularly in the parameter range of high-$\beta$ shock experiments. We find that there are three physical regimes exhibiting different nonlinear electron behavior depending on the relative size of the wavelength $\lambda$ of the turbulence compared with the electron gyroradius $r_e$. For high-$\beta$ shock experiments where $\lambda = 2\pi/k \ll r_e$, the electrons can be trapped in potential wells for longer than an electron gyroperiod, thus giving rise to a nonlinear electron-cyclotron instability which does not have the properties of the nonmagnetic ion-acoustic instability. This instability causes substantial electron heating and cross-field dif-

fusion corresponding to an effective electron-ion collision frequency of about $\omega_{pi}$ which persists well after a quasisteady level of turbulence is reached. In the second regime, $1 < kr_e < 2\pi$, the electrons are not as well trapped and the effective collision frequency is reduced. The third regime, $kr_e < 1$, will not be discussed. The second regime corresponds to the range of parameters studied in Ref. 4.

*Nonlinear theory.*—Since the numerical simulations indicate that nearly isolated potential wells exist for substantial lengths of time, insight into the nonlinear behavior of the electrons can be obtained from studying their motion in the combined electrostatic-magnetic potential wells of a wave, illustrated in Fig. 1. In the uniform magnetic field $B_z$, the constancy of the canonical momentum $P_y = m_e v_y + \Omega_e x$ implies that all electrons whose guiding centers are at $x = 0$ see the same $\vec{v} \times \vec{B}$ force which can be described by the potential $m_e \Omega_e^2 x^2/2$ given by the dashed line in Fig. 1. If we superimpose on this an electrostatic wave $\varphi \sim \exp i(kx - \omega t)$ moving from right to left for which $\lambda = 2\pi/k \ll r_e$, we obtain the combined potential $\Phi = -e\varphi + m_e \Omega_e^2 x^2/2$ shown in Fig. 1. In this phase plane the combined potential wells form to the right of $x = 0$, achieve their maximum depth as they move past $x = 0$, and become shallower and vanish to the left.

The linear growth of the waves will be significantly altered when electrons in resonance with the wave have been able to execute a trapping oscillation in a potential well. However, the presence of the magnetic field limits the time an electron can remain in resonance to either about $\Omega_e^{-1}$ or the time that a well in the combined potential $\Phi$ remains in existence, about $(e\varphi/m_e)(k/\Omega^2 v_d)$, whichever is shorter. Linear growth then will be

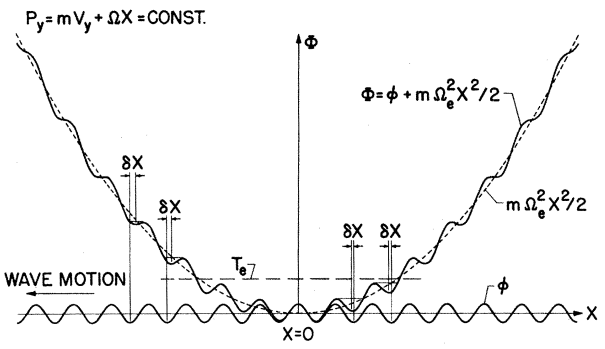


FIG. 1. The combined magnetic and electrostatic potential seen by electrons in the presence of a longitudinal electrostatic wave moving perpendicular to a fixed magnetic field.

modified when the minimum of these two times is longer than the trapping time $(m_e/e\varphi k^2)^{1/2}$ or

$$e\varphi/T_e \sim 1/(kr_e)^2. \quad (1)$$

Since typically $k\lambda_D \lesssim 0.5$ for maximum growth and $\lambda_D \ll r_e$, linear growth should be modified at a very low level. The field amplitude obtained in Ref. 4 for nonlinear modification is smaller by approximately $(kr_e)^{-1/2}$. However, once the electrons become trapped in the wells and $e\varphi/T_e \sim (kr_e)^{-1}$ so that the wells exist above the $T_e$ energy level, some electrons are carried to the left above the $T_e$ level before being released at a high energy into the larger magnetic well. Thus the electrons are heated with the energy going first into $v_y$ and then into $v_x$. In this situation the electron trapping time is considerably longer than a gyroperiod. If the potential well is stationary in its drifting frame, however, only a small fraction of electrons would be adiabatically trapped and there would be no increase in electron temperature. The adiabaticity is broken by fluctuations of the phase and amplitude of the potential wells themselves at a frequency comparable to the bounce frequency of electrons trapped in those wells. This bounce frequency is near $\omega_{pe}$. The mechanism is similar to that observed in the electrostatic bump-on-tail problem.[5] This nonadiabatic trapping acts as a diffusion and hence fills empty wells more efficiently than it empties full ones. Since the wells are not filled as efficiently as they would be in a growing potential in the absence of the magnetic field, the electron density maximum at the bottom of the wells is depressed from its value with $B = 0$. In addition, the perturbed charge density represented by the trapped electrons is shifted from the minima of the wells of $\varphi(x)$ by the displacements $\delta x$ in Fig. 1. The effect of this $\delta x$ is to shift the perturbed electron charge to the right relative to the charge density that would develop without the magnetic field. The ion charge density is almost entirely determined by $\varphi(x)$ alone. The phase shift and the reduced electron density maxima drive the nonlinear instability[2] to values of $\varphi$ much higher than that given by electron trapping alone.

The nonlinear electron heating rate due to the trapping and untrapping of electrons can be written as

$$\frac{dT_{e\perp}}{dt} = \frac{n_T}{n_0}\frac{m_e}{4}\frac{dv_T^2}{dt} = \frac{n_T}{n_0} v_{yT} \frac{m_e \Omega_e v_d}{2}, \quad (2)$$

where $n_T$ is the average density of trapped electrons in the plasma, $v_{yT}$ is the mean velocity of

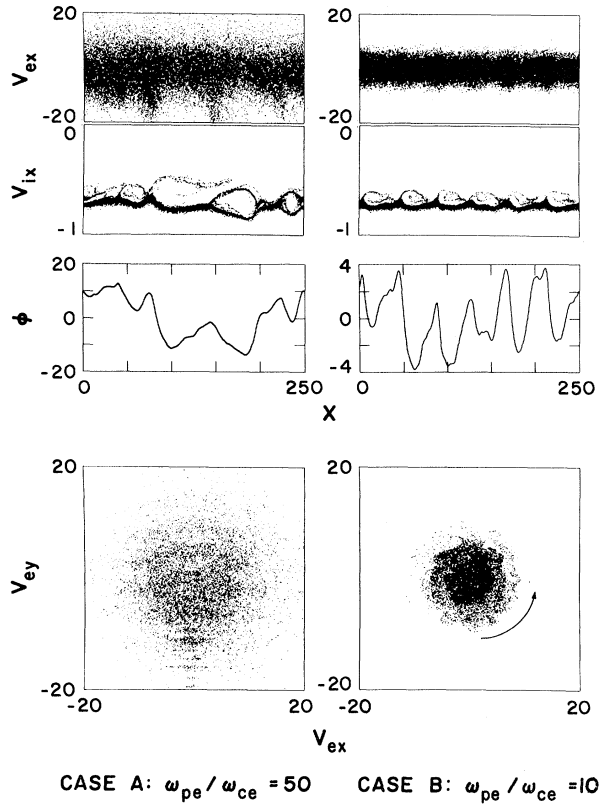


FIG. 2. Conditions in simulation plasmas at time $T=4000\omega_{pe}^{-1}$ for two cases differing only in the magnitude of the magnetic field.

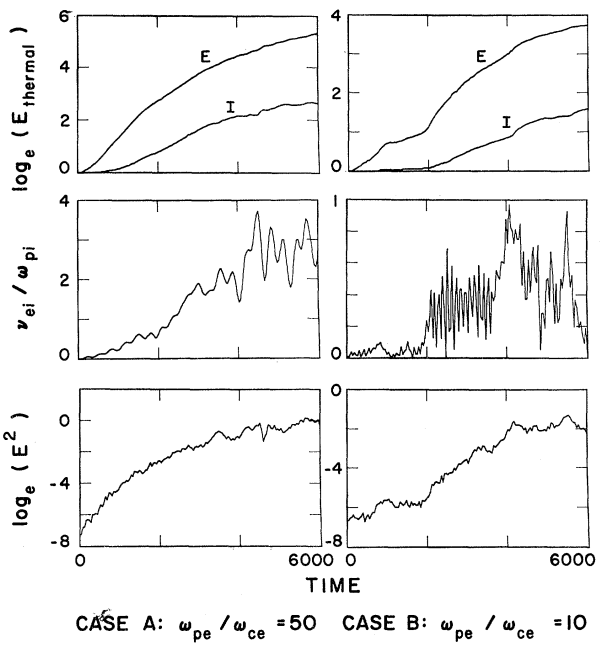


FIG. 3. Time histories for the simulation plasmas.

just the trapped electrons, and $dv_y/dt \simeq \Omega_e v_d$. Because of the nonadiabatic untrapping the maximum value of $v_{yT}$ should be considerably less than that implied by the vanishing of the wells. The quantity $v_{yT}n_T/n_0$ is just the net $v_y$ drift or resistive flow of the plasma across the magnetic field and can be measured directly from the simulations. The effective electron-ion collision frequency then is given by

$$\nu_{ei}=(\bar{v}_y/v_d)\Omega_e. \tag{3}$$

The ion heating rate in the strongly nonlinear regime is primarily due to the trapping of ions in the wave.

For $\omega_{pe}/\Omega_e \lesssim 10$, charge neutrality requires that $\lambda \gtrsim r_e$ and that the duration of electron trapping cannot become longer than the bounce time in the wells, thus significantly reducing the phase shifts which drive the nonlinear instability.

*Numerical simulations.*—The results of one-dimensional particle-in-cell[6] numerical simulations of the instability are summarized in Figs. 2 and 3 for $m_i/m_e=1836$, $T_e=\frac{1}{2}m_e v_{e0}^2=T_i=\frac{1}{2}m_i v_{i0}^2$, and $v_d=-0.75v_{e0}$ on a periodic grid of length $250v_{e0}/\omega_{pe}$ and two values of $\omega_{pe}/\Omega_e$, 50 for case A and 10 for case B. The simulations used 80 000 particles and 256 cells. Figure 2 shows the late-time evolution of the instability at $t=4000\omega_{pe}^{-1}$ for the two values of the magnetic field. The plots from top to bottom are $v_y$ vs $x$ for the electrons, $v_x$ vs $x$ for the ions, both in units of $v_{e0}$, $\varphi(x)$ in units of $m_e v_{e0}^2/2$, and $v_y$ vs $v_x$ of a set of electron test particles in the $P_y=0$ phase plane. The downward fingerlike projections in case A are electrons with large negative $v_y$ velocities trapped in the corresponding potential well. The bottom frame shows a cross section of these fingers in the $P_y=0$ plane. These stripes correspond to vortices of electrons trapped in the combined potential wells. They move from top to bottom of the figure with velocity nearly equal to $v_d$, entering without electrons, filling near the middle as described above, and moving out the bottom carrying trapped electrons which then come out of the vortices with a larger velocity of gyromotion. In the quasistationary state the energy supplied to the electrons comes from the breaking of the ions in $v_x$-$x$ space. As the heating continues, the turbulence evolves to longer wavelengths corresponding to $kv_e/\omega_{pe}\sim 0.5$.

Case B with $\omega_{pe}/\Omega_e=10$ shows quite different behavior. The Debye length cutoff requires $\lambda \gtrsim r_e$ so that the electrons are not trapped efficiently in the potential wells, but rather show a

somewhat ordered lumpy structure in the $v_x$-$v_y$ plot of Fig. 2. Nevertheless, the instability has evolved to a strongly turbulent level even though initially $T_e = T_i$.

A summary of the time evolution of the two cases in shown in Fig. 3 with plots of four average quantities: the average kinetic energies $T_e$ and $T_i$ for electrons and ions about their respective mean velocities, the instantaneous electron-ion collision frequency defined by Eq. (1), and the total electric field energy $\sum_k E_k^2$. For case A the initial fluctuation level is above that at which the electrons are nonlinearly affected by the wave so the linear instability is not seen. The nonlinear instability is observed to grow, however, even though the ratio of $T_e/T_i$ is too small for there to be any instability in the absence of the magnetic field. Clearly the growing waves do not satisfy the nonmagnetic ion-acoustic dispersion relation. In support of this, the wave velocity has been measured at least during the phase of rapid growth to be considerably faster than the ion-acoustic speed. The electron-ion effective collision frequency is the Coulomb collision value at early time, $\nu_{ei} \sim 0.02\omega_{pi}$, but increases by 2 orders of magnitude to about $2\omega_{pi}$ by time $3000\omega_{pe}^{-1}$. After a quasisteady level determined by strong ion trapping is reached, the effective collision frequency does not change substantially until late in the problem where the waves become box limited. By the time $8000\omega_{pe}^{-1}$ the electron energy has increased 260 times, taking about 30% of the drift energy from the ions.

For case B a "saturation" of the linear instability is observed at time $1000\omega_{pe}^{-1}$ which corresponds about equally well to the "knee" of Ref. 4 or to the trapping level of Eq. (1). However, at time $2000\omega_{pe}^{-1}$ the nonlinear electron-cyclotron instability again begins to grow despite the fact that the nonmagnetic ion-acoustic dispersion relation for the existing conditions does not predict instability. Thus the nonlinear instability grows even without efficient electron trapping for $T_e \sim T_i$ and $v_d < v_e$. By time $6000\omega_{pe}^{-1}$ the electron energy has increased by a factor of 40, absorbing about 5% of the initial ion drift energy. The effective collision frequency increases from its collisional value to about $0.5\omega_{pi}$ by time $2500\omega_{pe}^{-1}$ and remains relatively steady with oscillations near the electron-cyclotron frequency. The heating rate is distinctly slower than in case A. Nevertheless, for both cases $T_e/T_i$ seems to approach ~10. The various properties of the quasisteady state reached here are quite insensitive to the initial $T_e/T_i$ but depend quite sensitively on the value of $\omega_{pe}/\Omega_e$.

To summarize, it has been shown that quite distinct from the linear electron-cyclotron drift instability, a nonlinear electron-cyclotron instability exists for field amplitudes large enough to trap electrons. In weak magnetic fields this nonlinear instability can give rise to a large anomalous resistance to perpendicular currents for times at least as long as $200\omega_{pi}^{-1}$. The mechanism is simply the pulling of clumps of trapped electrons across the magnetic field by the drifting density maxima of the ions. The trapped electrons pull back against the ion drift, thus causing the ions to lose drift energy and gain a little thermal energy by breaking, while the electrons themselves are heated by increasing their $v_y$ until they are pulled out of the potential wells. If the magnetic field is sufficiently strong, the electrons are not trapped efficiently and the resistance drops.

The nonlinear model of Ref. 4 of resonance broadening due to a random-phased turbulence is probably just the incoherent analog of the onset of trapping at small field amplitudes described earlier. However, we conclude that this resonance model does not accurately describe the further evolution of the instability to highly nonlinear field levels. First, the nonlinear instability does not behave like the nonmagnetic ion-acoustic instability since it can occur for $T_e \sim T_i$ and $v_d < v_e$ and the final nonlinear state depends critically on the size of the magnetic field. Second, the heating rate is not observed to decrease significantly after the quasisteady turbulent state is reached. That is, ion trapping does not reduce the effective resistance. Third, consistent with this steady heating rate, in the presence of a weak magnetic field a large fraction of ion streaming energy can be converted to electron thermal energy.

This work was performed under the auspices of the U. S. Atomic Energy Commission.

[1]D. W. Forslund, R. L. Morse, and C. W. Nielson, Phys. Rev. Lett. 25, 1266 (1970).

[2]D. W. Forslund, R. L. Morse, and C. W. Nielson, "Theory of Turbulent Heating and Anomalous Diffusion in Pinch Plasmas," IAEA Conference Paper, 1971 (to be published).

[3]M. Keilhacker and K. H. Steuer, Phys. Rev. Lett. 26, 694 (1971).

[4]M. Lampe, W. M. Manheimer, J. B. McBride, J. H. Orens, R. Shanny, and R. N. Sudan, Phys. Rev. Lett.

26, 122 (1971).
[5]R. L. Morse and C. W. Nielson, Phys. Fluids 12, 2418 (1969).
[6]R. L. Morse, in *Methods in Computational Physics*, edited by B. Alder, S. Fernbach, and M. Rotenberg (Academic, New York, 1970), Vol. 9, p. 213.

# Generation of Astron-Type $E$ Layers Using Very High-Current Electron Beams*

M. L. Andrews,† H. Davitian, H. H. Fleischmann, B. Kusse, R. E. Kribel,‡ and J. A. Nation
*Laboratory for Plasma Studies and Department of Applied Physics, Cornell University, Ithaca, New York 14850*
(Received 20 May 1971)

Reversal of the axial magnetic field in a magnetic-mirror trap is achieved by injection of a 30-kA, 0.34-MeV beam of electrons.

In 1958, Christofilos suggested[1] that stable confinement of a fusion plasma could be attained by injecting a cylindrical layer of highly relativistic electrons into a magnetic-mirror field. If this "$E$ layer" is sufficiently strong to reverse the direction of the magnetic field on the cylinder axis, the magnetic field in the vicinity of the layer will constitute an absolute-minimum-$B$ configuration with closed field lines. This suggestion led to the well-known Astron experiments which attempt to create such current layers by injection of a low-angular-divergence beam of relativistic electrons. After considerable technological developments, it has been found that single-pulse trapping of an 800-A, 6-MeV electron beam leads to $E$ layers exhibiting axial-field changes of up to 13% and stable confinement of up to 12 msec.[2] However, to attain full field reversal, the stacking of a sequence of pulses appears necessary.

On the other hand, as a result of recent advances in high-voltage technology, pulsed electron beams of up to several hundred kiloamperes and several MeV are now available which may be used for single-pulse generation of strong $E$ layers. The angular divergence of these beams exceeds that of the Astron beam; the influence of the angular divergence on injection may be balanced by the magnetic self-focusing of the beam.[3-5] When trapped, this increased perpendicular energy can be expected to result in a more stable $E$ layer of larger useful volume.[6] In this paper, first results of some small-scale experiments are reported in which full field reversal was obtained for a short time period.

In these experiments, electron beams of 30–60 kA, having energies of 300–500 keV and a pulse duration of 50 nsec, were generated in the Cornell electron-beam facility.[7] As indicated in Fig. 1, these beams were guided through a soft-iron injector tube having 4 cm i.d., 1.10 m length, and 4 mm wall thickness. From this tube, the beam was injected into a Lucite tank, 25 cm in diameter and 1.80 m in length. Injection angle relative to the tank axis and injection radius could be varied from 75° to 90° and 6 to 10 cm, respectively. The tank was lined with a copper screen electrically connected to the injector and to a metal flange at the downstream end of the tank. Upstream, the tank was sealed with a transparent Lucite flange. A uniform magnetic field parallel to the tank axis was generated by coil windings (2 per in.) around the tank wall. In addition, movable field coils provided the capability for local field enhancements. The field energy was supplied by a capacitor bank having a quarter-cycle rise time of 3.4 msec. Gas pressures from 0.1 to several Torr were maintained in the tank.

For diagnostic purposes, open-shutter cameras viewed the tank from the side and through the Lucite flange at the upstream end. Fast changes of the axial magnetic field were measured by three magnetic pickup coils. Two of these coils could be moved along the tank axis entering from opposite ends, while the third could probe the field at various radial positions. Each probe consisted of an electrostatically shielded ten-turn loop of 0.007-in. copper wire wound on $\frac{1}{4}$-in. Lucite cylinders and placed in glass tubes having a $\frac{1}{2}$-in. o.d. Their output signals were fed through terminated 50-$\Omega$ cables, integrated by low-inductance, 10-$\mu$sec $RC$ integraters, and finally displayed on scopes. The effectiveness of the electrostatic shielding and the general noise level were tested by placing all three probes in adjacent positions on axis. As expected, two identically wound axial probes showed signals of opposite